

Electronically Tuned Phase Transition in Germanium Telluride (GeTe) Cells for Memory and RF switch Applications

Dushyant Tomer¹, and Ronald A. Coutu, Jr.^{*1}

Department of Electrical and Computer Engineering, Marquette University, USA

Abstract: Germanium telluride (GeTe) is a phase change material that undergoes an amorphous to crystalline transition upon heating to $\sim 200^{\circ}\text{C}$. This transition is reversible in nature and results in \sim six orders of magnitude difference in GeTe resistivity which makes it a suitable candidate for data storage and other functional devices. In this work, micro-size phase change test cells were fabricated by RF sputtering GeTe thin films onto silicon (Si) wafers and Si wafers coated with silicon dioxide (SiO_2), silicon nitride (Si_3N_4), and alumina (Al_2O_3) films. Two different heating methods, conductive and electrical (i.e., Joule heating), were applied to induce the phase transition mechanism in the GeTe cells. The phase change, obtained from two different heating methods, was investigated using spectroscopic ellipsometry, thermal, electrical and radio-frequency methods. It was observed in ellipsometry that the extinction coefficient, hence the absorption coefficients of GeTe cells increases with amorphous to crystalline phase change. Furthermore, an optical contrast of $\Delta n + i\Delta k = -0.858 + i1.056$ was also recorded suggesting a sharp transition between phases. In addition, a growth dominated crystallization and fracturing of conductive crystallites when deposited on Al_2O_3 was noticed in the thermal experiments. A current-voltage (I-V) characteristic, similar to a memory-type device, was observed during the electronic experiments. Finally, radio frequency (RF) measurements were performed on GeTe cells to investigate the capability of being utilized as improved RF switches.

Key words: phase change materials, electronic memory, germanium telluride, RF switching

1. Introduction

Chalcogenide-based phase change materials (PCM) have been used in optical such as CD/DVD and digital memory applications since their discovery [1-3]. The amorphous and crystalline phases of a PCM material possess different band structures resulting in significant distinction in optical and electrical properties [1-3]. Germanium telluride (GeTe) one of the most promising PCM material shows amorphous to crystalline phase transition at $T \sim 180^{\circ}\text{C}$ [4]. Associated with temperature induced crystallization is an increase

in reflectivity which has been exploited in CDs, DVDs, and Blu-ray discs. In such applications, laser pulses are used to supply heat for initiating the phase transition. Similarly, six orders of magnitude difference between amorphous and crystalline phase resistivity of GeTe has been reported [4]. Such large and sharp resistivity difference results in intrinsic binary states (i.e. “1” and “0” or “ON” and “OFF” states) which can be utilized in digital storage applications if a fast method for crystallization and re-amorphizing is known. Furthermore, very small (near metal-like) resistivity of crystalline GeTe can be used in fabrication of high performance RF switches and related technologies [5, 6]. However, phase transition required for memory and RF applications cannot be achieved by laser heating due to complicated device structures and need of large

Corresponding author: Ronald A. Coutu, Jr., Ph.D., P.E., Professor of Electrical and Mechanical Engineering; areas/interests: microelectromechanical systems (MEMS), device fabrication, micro-electrical contacts. E-mail: Ronald.Coutu@marquette.edu.

scale uniform heating. Therefore, researchers and scientists have refocused on other heating methods so that large resistance contrast can be achieved.

One such method is heating the PCM device using voltage pulses of sufficient energy. Under the influence of voltage pulsing, PCM device temperature goes beyond the glass transition point and starts the crystallization [7]. In the beginning of crystallization process only small nuclei form but their coalescence with each others at higher temperature completes the transition. Depending on the PCM, such phase transition can be either growth-dominated where the crystallites grow at the interfaces of the material or nucleation-dominated materials where crystallization begins primarily in the inner bulk of the material [7]. Therefore, voltage pulse with different parameters are required to induce phase transition in different materials. For GeTe thin films, a longer duration current pulse to heat the amorphous phase material above its crystallization temperature to induce recrystallization, whereas a higher magnitude current pulse with shorter duration can bring the material back to amorphous phase after melting and quenching process

In comparison of amorphous phase (a-GeTe), more research has been done on the crystalline phase GeTe (c-GeTe) which explains many interesting properties found in the literature [8-10]. For example, p-type conductivity in “as-grown” GeTe films is attributed to the presence of Ge vacancies contributing two holes to the valence band. Furthermore, low formation energy of these vacancies is responsible for nanosecond switching time and reversible phase change in the whole volume. On the other hand, the less studied a-GeTe shows complex conductivity (or resistivity) behavior. From the initial highly resistive state, conductivity increases linearly until a threshold point is reached, when the conductivity increases exponentially. This threshold switching is critical for amorphous (highly resistive) PCM as it reduces the current required to heat the PCM cell to its crystalline state

[11]. This low power consumption is a major concern for battery-powered RAM in the future.

This paper demonstrates GeTe thin films in phase change random access memory (PCRAM) and RF switch applications. GeTe devices of different geometries and dimensions were designed and fabricated on various supporting substrates using standard UV-photolithography. The optical response of these devices was investigated using spectroscopic ellipsometry. In thermal measurements, substrate dependent volatile and nonvolatile change in resistance were recorded. Furthermore, a PCRAM type current-voltage behavior was recorded for GeTe cells which confirms their use in memory applications. Finally, a radio frequency (RF) characterization of GeTe switches was done using a two-port switch architecture. It was discovered that the intrinsic ON and OFF properties in the crystalline and amorphous material phases make GeTe an excellent candidate for RF switching applications.

2. Device Fabrication and Characterization Methods

2.1 Fabrication

In this work, standard photolithography processes were used to fabricate micro-size GeTe phase change cells on different substrates, (e.g., silicon (100), SiO₂/c-Si, Si₃N₄/c-Si and c-Al₂O₃). The silicon dioxide and silicon nitride substrates were prepared by depositing 300 nm thick SiO₂ and 100 nm thick Si₃N₄ film on c-Si using thermal oxidation and plasma enhanced chemical vapor deposition (PECVD), respectively. The optical microscope images of as-fabricated devices are shown in Fig. 1(a-c). The device shown in Figure 1(a) consists of a GeTe strip of dimensions 10 μm × 30 μm, while a longer GeTe strip of width 10 μm connects the metal contacts of device viewed in Fig. 1(b). The RF switch structure is also shown in Fig. 1(c). All the devices have two common components, bi-metallic contact pads and a GeTe bridge connecting the two contact pads. The GeTe

connecting layer of thickness ~ 100 nm was deposited by RF sputtering (300 W power, 10 mTorr growth pressure with 20.1 sccm Ar flow) of a high purity GeTe target for 2 minutes. It is noteworthy to mention that GeTe deposition was done on room temperature substrates to make sure its amorphous nature in as grown films. On the other hand, metal contacts

consisting of 10 nm Ti and 100 nm Au were deposited in high vacuum E-beam evaporation system. The Ti layers known to improve the adhesion between gold and substrate are crucial for good and stable electrical contacts. A lift-off process using acetone was performed to remove the extra material.

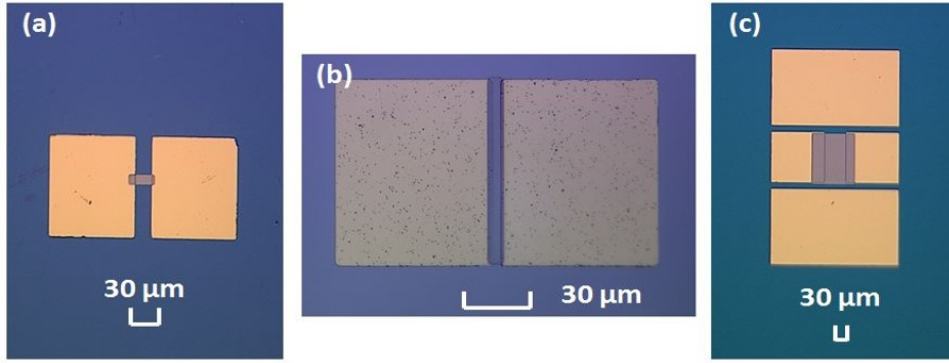


Fig. 1 Optical microscope image of (a) a PCM device consisting GeTe strip of dimensions $10 \mu\text{m} \times 30 \mu\text{m}$, (b) a smaller device with $10 \mu\text{m}$ width (used for I-V measurements on sapphire substrate) and (c) a RF resistor consisting of top and bottom ground lines and a middle signal line.

2.2 Spectroscopic Ellipsometry

The amorphous and crystalline phase GeTe thin films were first investigated by spectroscopic ellipsometry (SE). The experimental SE data can be expressed by two parameters Δ (phase shift between incident and reflected light) and Ψ ($\tan \Psi$ tells about amplitude change upon reflection). The fundamental equation of ellipsometry correlates these two parameters with total reflection coefficient \mathcal{R} as [12],

$$\rho = \tan \Psi e^{j\Delta} = \frac{\mathcal{R}_p}{\mathcal{R}_s} \quad (1)$$

The interaction with sample surface decomposes the incident light into two components “p” and “s”, where p- oscillates parallel to the plane of incidence light and the s- oscillates parallel to the sample surface (or perpendicular to the incident light). In literature, many models have been applied on Eq. (1) to obtain characteristic parameters of a material such as the index of refraction n , the extinction coefficient k , and the film thickness d . However, only two widely used models, Tauc-Lorentz dispersion [13] and classical [14], were used to explain the behavior of amorphous

and crystalline GeTe, respectively. The Tauc-Lorentz dispersion model combines the Tauc joint density of states with the Lorentz oscillator. Therefore, the complex dielectric function, $\epsilon = \epsilon_r + i\epsilon_i$, can be expressed as [13]

$$\epsilon_i(E) = \begin{cases} \frac{1}{E} \frac{A E_0 C (E - E_g)^2}{(E^2 - E_0^2)^2 + C^2 E^2} & E > E_g \\ 0 & E \leq E_g \end{cases} \quad (2)$$

$$\epsilon_r(E) = \epsilon_\infty + \frac{2}{\pi} P \int_{E_g}^{\infty} \frac{\xi \epsilon_i(\xi)}{\xi^2 - E^2} d\xi \quad (3)$$

where A is the peak strength, C the broadening term, E_g the bandgap energy, and E_0 the position of the peak (all in Eq. (2)). While, ϵ_∞ is the high frequency dielectric constant and P the Cauchy principal part of the integral of Eq. (3). On the other hand, the classical dispersion model based on the sum of the single and double Lorentz and Drude oscillators can be expressed by [14]

$$\epsilon(\omega) = \epsilon_\infty + \frac{(\epsilon_s - \epsilon_\infty)\omega_p^2}{\omega^2 - \omega_0^2 + i\Gamma_0\omega} + \frac{\omega_p^2}{-\omega^2 + i\Gamma_D\omega} + \sum_{j=1}^2 \frac{f_j \omega_j^2}{\omega_j^2 - \omega^2 + i\gamma_j\omega} \quad (4)$$

where the first term is the high frequency dielectric

constant, second term is the Lorentz oscillator, third is the Drude oscillator, and fourth term is for two extra oscillators, if needed. The parameters describing the real part of the dielectric function are ϵ_∞ (high frequency dielectric constant) and ϵ_s (static dielectric function). The difference $\epsilon_s - \epsilon_\infty$ represents the strength of a single Lorentz oscillator. The parameters describing the imaginary part of dielectric function are ω_l (resonant frequency of a Lorentz oscillator), and Γ_l (damping factor of a Lorentz oscillator). At the end, the important parameters from the fourth term are f_j (oscillator strength), ω_j (resonant peak energy of an oscillator), and γ_j (broadening parameter corresponding to the peak energy of each oscillator).

2.3 Thermal Characterization

As mentioned in the introduction, when transitioning phase using a laser only a small section of material crystallizes (i.e., only the laser spot size area shows phase transition upon exposure). Therefore, laser heating is not the first choice for either memory or RF switching applications. In contrast, conduction heating uniformly increases the temperature of the whole sample resulting in greatest change in the GeTe resistivity. In this work, GeTe phase transition was demonstrated using a customized setup which increased device temperature through conduction. This measurement setup consists of a probe station thermal chuck, a brass platform, a ceramic plate, a thermocouple, a voltage source meter, and digital multimeter. The devices were sandwiched between brass (bottom) and ceramic (top). This ceramic plate minimizes the air flow in proximity of devices and reduces the heat dissipation. A thermocouple was also mounted in the sandwich structure for precise temperature measurement. This whole setup was placed directly onto the thermal chuck. The metal to metal (i.e., thermal chuck and brass) contact conducted the heat faster. The temperature dependent current-voltage behavior of GeTe devices was measured using a digital multimeter and a source meter.

2.4 Electrical Characterization

It is also suggested that short power pulses of large enough magnitude can also induce reversible phase transition in GeTe devices. A voltage pulse of long enough duration sets the PCM material in ON states (crystalline) and the rapid removal of pulse brings it back to OFF (amorphous) state. Such pulse induced ON and OFF states are useful in storing data in bit form. Furthermore, voltage pulsing offers fast switching action; typically, 10 ns from OFF to ON and ~ 5 ns from ON to OFF state [15]. In this work, voltage pulsing was done using a DC source and current (pulse height) was measured using a digital multimeter.

2.5 RF Switching

The S parameters of GeTe devices were obtained in the frequency range of 10 MHz to 20 GHz using a two-port RF network. Such parameters can be defined as [16]

$$\begin{bmatrix} V_1^- \\ V_2^- \end{bmatrix} = \begin{bmatrix} S_{11} & S_{12} \\ S_{21} & S_{22} \end{bmatrix} \begin{bmatrix} V_1^+ \\ V_2^+ \end{bmatrix} \quad (5)$$

where V_i^- terms are wave components traveling away from the i^{th} port, and V_i^+ terms are wave components traveling towards the i^{th} port. Therefore,

$$S_{11} = \left. \frac{V_1^-}{V_1^+} \right|_{V_2^+=0} \quad \text{and} \quad S_{21} = \left. \frac{V_2^-}{V_1^+} \right|_{V_2^+=0} \quad (6)$$

where S_{11} is the reflection coefficient for port 1, and S_{21} is the insertion loss from port 1 to port 2. Due to bi-directional network, $S_{11} = S_{21}$. Therefore, the experimental data of all the devices is presented in the form of S_{11} and S_{21} only. In this work, RF testing of GeTe switches was done using a high frequency network analyzer.

3. Results and Discussion

3.1 Spectroscopic Ellipsometry

The SE measurements on amorphous (a-) and crystalline (c-) GeTe cells were performed in the

spectral range of 1.50-6.50 eV at intervals of 0.05 eV. The index of refraction (n) and the extinction coefficient (k) for a-GeTe and c-GeTe were extracted using the Tauc-Lorentz and the Classical model, respectively. The extracted n and k values are shown in Fig. 2(a-d). The observed increase in k value upon transitioning from amorphous to crystalline phase [blue

lines in Fig. 2(a) and (b)] is a clear indicative of increased absorption primarily in the infrared wavelengths. The Lambert's law of absorption gives a relation between α with k :

$$k = \frac{\lambda}{4\pi} \alpha \quad \text{and} \quad I(z) = I_0 e^{-\alpha z} \quad (7)$$

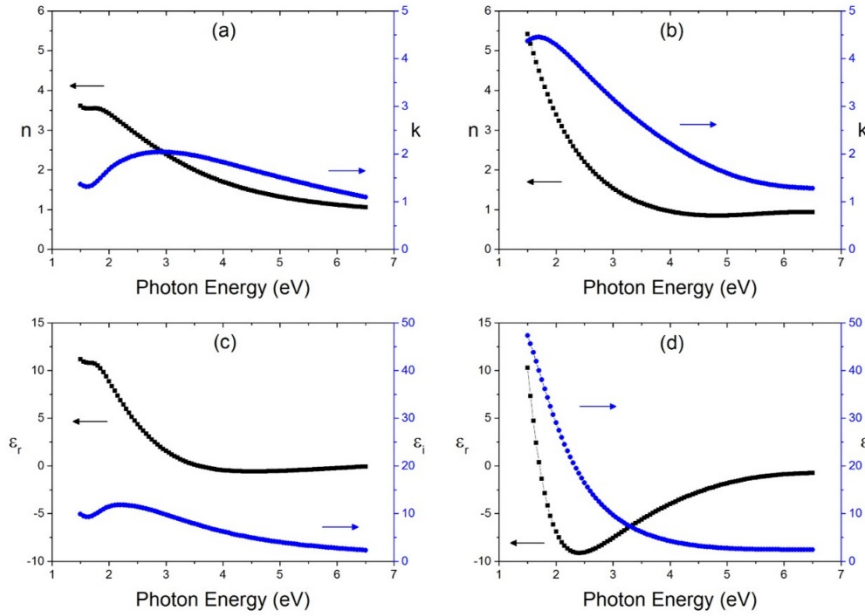


Fig. 2 (a) and (b) show index of refraction (n) and extinction coefficient (k) versus photon energy plots for amorphous and crystalline GeTe thin films, respectively. Similarly, (c) and (d) represent real and imaginary parts of the complex dielectric function for amorphous and crystallite GeTe thin films, respectively.

where I_0 and $I(z)$ represent the intensity of the incident light at the surface and at the depth z inside the sample, respectively. In c-GeTe, the largest k value (~ 5.4) was recorded at 1.75 eV (709 nm) giving maximum value of absorption coefficient $\alpha = 9.56 \times 10^5 \text{ cm}^{-1}$. With the constant absorption coefficient, the intensity of incident light reduces by a factor of 5.60×10^{-9} at 200 nm depth from its original value (at $z = 0$ nm). Furthermore, Fig. 2 (a) and (b) also quantify the contrast for optical phase change media by using $\Delta \tilde{N} = \Delta n + i\Delta k$, where Δn and Δk were obtained by subtracting amorphous n and k values from the corresponding crystalline phase values. The real and imaginary parts of complex dielectric function of a- and c-GeTe, respectively, are shown in Fig. 2(c) and (d). A broad ϵ_i peak was seen for a-GeTe which corresponds to a smearing of electronic states (i.e.,

dielectric relaxation). However, the improvement in crystallinity of the film decrease the electron scattering and increase the free-electron density as shown in Fig. 2(d). These data are in good correspond to other FTIR experiments where the broadband absorption increases from amorphous to crystalline phases along the infrared spectra. Additionally, the *in-situ* rate of increase in absorption seems to proportionately follow the rate of decrease in resistivity a monotonic relationship with the largest change occurring at the glass temperature.

3.2 Thermal Characterization

Semi-logarithmic R versus T plots of four different GeTe devices are shown in Fig. 3(a-d). A nonvolatile transition in which device resistance never come back to its initial value was observed for GeTe films

deposited on dielectric material (i.e., thermal SiO₂ and Si₃N₄) coated c-Si substrates. Such permanent change is shown in Fig. 3(a) and (b). However, a volatile phase transition was recorded for GeTe deposited directly on c-Si and Al₂O₃ substrates. The corresponding results presented in Fig. 3(c) and (d) show that the device resistance recovers back to its initial value. Here, all the devices but GeTe/c-Si exhibit six orders of magnitude change in resistance, GeTe/Al₂O₃ samples have greatest initial resistance (~ 10⁹ ohms). Such behavior

cannot be explained by the thin film stoichiometry or interaction between the substrate and the thin films. A much better approach is to consider heat induced phase transition where heat transfer via conduction through one material, q_1 , and through two materials, q_2 , can be defines as [17]

$$q_1 = \frac{T_H - T_{L1}}{\left(\frac{d}{kA}\right)} \quad \text{and} \quad q_2 = \frac{T_H - T_{L2}}{\left(\frac{d_1}{k_1 A_1} + \frac{R_i}{A_i} + \frac{d_2}{k_2 A_2}\right)} \quad (8)$$

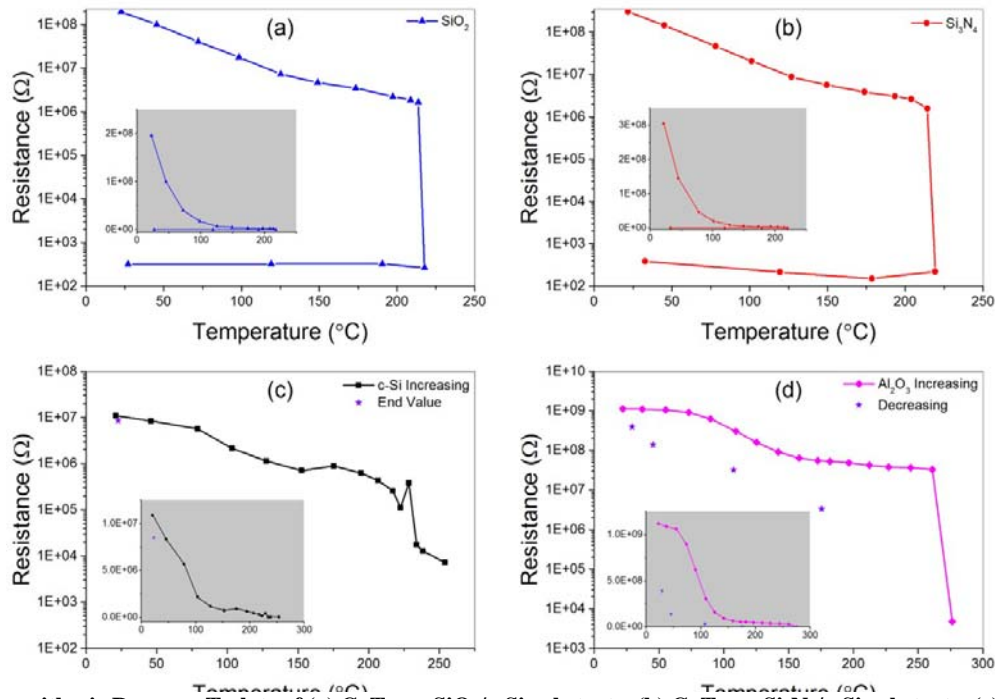


Fig. 3 Semi-logarithmic R versus T plots of (a) GeTe on SiO₂/c-Si substrate, (b) GeTe on Si₃N₄/c-Si substrate, (c) GeTe on c-Si substrate, and (d) GeTe on Al₂O₃ substrate. The top plots show a nonvolatile change in resistance indicative of permanent crystallization; the bottom plots show a volatile transition (Inset show the resistance versus temperature data on linear scale).

where T_H is the high temperature, T_L the low temperature, d the thickness of the material, k the thermal conductivity of the material, A the cross-sectional area of heat conduction, and R_i the interfacial thermal resistance between the two materials. Here, the denominator terms d_l/k_l represents the thermal resistance R_l for the l^{th} layer in units of m²KW⁻¹. For dielectric coated substrates, R_{tot} can be defined as the sum of the two layers' resistances and the interfacial resistance. However, it would be simply d/k for c-Si and Al₂O₃ substrates.

The total thermal conduction (G_{tot}) of all tested

samples is given in Table 1. Among all devices, GeTe/c-Si substrate shows largest G_{tot} which confirms the results shown in Fig. 3; GeTe/c-Si samples have least resistive conduction path. Furthermore, Fig. 3 provides important information regarding the conduction heat induced crystallization in GeTe thin films. As thermal chuck source was beneath the devices, heat moves in vertically upward direction only. This upward heat flow from substrate to GeTe film via dielectric layer results in to the formation of small crystallites responsible for resistance decrease. Fig. 3 (a, b and d) are typical I-V behavior resulting from the

crystallization process. However, higher conductivity of c-Si substrate allows the formation of such crystallites at lower temperature and eventually results in to lower initial resistance with smooth phase

transition (Fig. 3(c)). The small resistance change (10^3 ohms) makes GeTe/c-Si less useful despite showing volatile transition.

Table 1 Heat conduction parameters (blank values are N/A).

Material	d [m]	k [$Wm^{-1}K^{-1}$]	R_i [m^2KW^{-1}]	R_{tot} [m^2KW^{-1}]	G_{tot} [$Wmm^{-2}K^{-1}$]
SiO ₂	300×10^{-9}	1.4 ⁽²⁶⁾		214×10^{-9}	
Si ₃ N ₄	100×10^{-9}	0.03 ⁽²⁷⁾		33.3×10^{-6}	
c-Si	500×10^{-6}	141.2 ⁽²⁸⁾		35.4×10^{-6}	0.28
Al ₂ O ₃	432×10^{-6}	35 ⁽²⁹⁾		12.3×10^{-6}	0.08
SiO ₂ /c-Si			1.78×10^{-6} ⁽²⁹⁾	5.54×10^{-6}	0.18
Si ₃ N ₄ /c-Si			2.25×10^{-6} ⁽²⁷⁾	9.12×10^{-6}	0.11

The crystallization process in GeTe/Al₂O₃ samples look normal as resistance is decreasing with increasing the temperature. These samples demonstrate the reverse phase transition, i.e., crystalline to amorphous, with decreasing temperature. Fig. 3(d) shows that the resistance return to the initial value, however, through a different path. This different path suggests that crystalline to amorphous transition is much slower than the transitioning between amorphous to crystalline. Such ambiguity can be explained by considering the thermal expansion coefficients. These coefficients (units of $10^{-6}/^{\circ}C$) for Al₂O₃ and GeTe are 5.3 and 0.56, respectively. This one order of magnitude difference in thermal expansion between Al₂O₃ and GeTe may cause fracturing of the conductive crystallites within the thin film during cooling process.

3.3 Electrical Characterization

The current-voltage (I-V) characteristic of GeTe cells is shown in Fig. 4(a-d). Here, Fig. 4(a) shows the I-V behavior of just bare substrates. Similar to thermal measurements, c-Si and Al₂O₃ substrates were found least and most resistive, respectively, in electrical measurements. The c-Si substrate shows large current (~ 0.1 A) at small bias voltage (~ 18 V), whereas negligible current (\sim few μ A) was recorded for dielectric substrates even at 75 V. Here, GeTe/c-Si mimics a typical I-V curve of a PCRAM as shown in Fig. 4(b). The conductivity was found to increase

linearly and then exponentially until it reaches a threshold voltage, V_t , between 30 V and 30.8 V. An inward snap of the I-V curve was apparent, whereby the voltage in the cell was reduced and the current increases (i.e., large increase in conductivity). The subsequent voltage is called the holding voltage, V_h [18]. Once it is reached, the current increases with very little change in V_h ; however, some negative differential resistance (i.e., NDR) is seen in this region as well. The high current provides enough Joule heating to crystallize the GeTe thin film. Once the power is reduced, the conductivity is ohmic due to the crystallization. These observations match those of Ielmini and Zhang based on their analytical model of subthreshold switching in chalcogenides. In their model, the current I in the subthreshold region is expressed as [19]

$$I = 2qAN_{T,tot} \frac{\Delta z}{\tau_0} \exp\left(-\frac{E_C - E_F}{kT}\right) \sinh\left(\frac{qV_A \Delta z}{kT 2u_a}\right) \quad (9)$$

where q is the electron charge, A the cross-sectional area of the PCM cell, $N_{T,tot}$ the integration of the trap distribution above the Fermi level, Δz the intertrap distance, τ_0 the characteristic attempt-to-escape time for a trapped electron, E_C the conduction band energy, E_F the Fermi level, kT the thermal energy, V_A the applied voltage, and u_a the thickness of the PCM cell from one electrode to the other. The \sinh term comes from a balancing of forward and reverse current

which is important for small V_A (recall that $2 \sinh x = e^x - e^{-x}$). Furthermore, $E_C - E_T$ representing the barrier height between two donor-like traps is reduced by magnitude ΔU in the presence of an electric field F . As the field increases, the barrier is reduced and electrons flow into the conduction band via thermal

emission over the barriers or by direct tunneling through the barriers. This barrier height reduction can be expressed as [19]

$$\Delta U \approx -qF \frac{\Delta z}{2} = -q \frac{V_A}{u_a} \frac{\Delta z}{2} = -qV_A \frac{\Delta z}{2u_a} \quad (10)$$

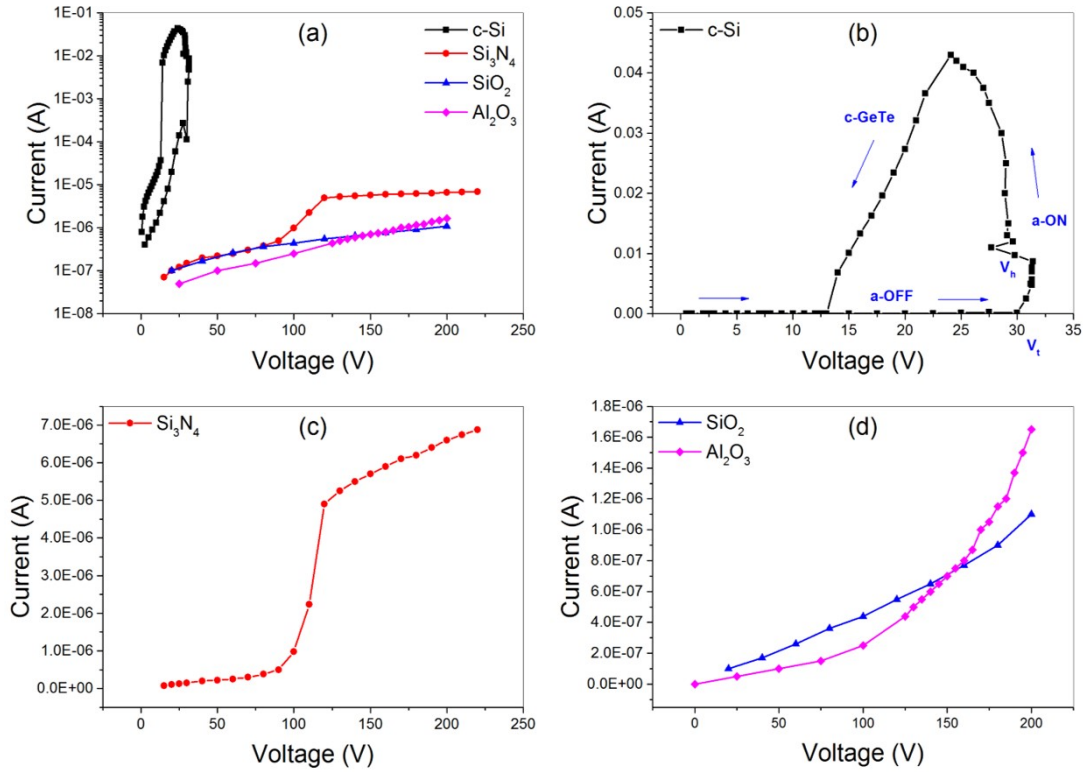


Fig. 4 (a) Semi-logarithmic I-V plots of all four samples for comparison, (b) memory curve of GeTe/c-Si substrate showing amorphous ON and crystallization, (c) GeTe on Si₃N₄/c-Si substrate, and (d) SiO₂/c-Si and Al₂O₃ plots which do not reach an amorphous ON state.

One important observation is that this model is valid for vertically integrated PCM cells where the electrodes are above and below the chalcogenide material. Therefore u_a is both the thickness of the thin film and the distance between electrodes (~ 30 nm). As u_a increases, resistance increases, subthreshold slope of current decreases, and threshold voltage increases.

Based on this relationship between u_a and conductivity, the results in Fig. 4 can be explained. In the c-Si case, the effective u_a is decreased due to partial crystallization of the bottom portion of GeTe. It can be assumed that there are pockets of crystalline areas because the heat transferred during fabrication was not great enough to create a solid crystalline film.

However, u_a is too large to generate substantial current in other cases (Fig. 4(c-d)). Furthermore, the starting resistance was an order of magnitude larger than c-Si, the subthreshold slope was shallow, and the threshold voltage was not reached; however, NDR is visible in all three cells. These non-idealities do not mean that amorphous chalcogenides cannot be used for threshold switching. If u_a was shorter (~ 1 μ m), typical memory curves like Fig. 4(b) would be expected with a smaller threshold voltage ($F = V_A/u_a$). The horizontal design is simpler than the vertical design because it requires fewer lithography steps and fewer requirements are placed on the electrode materials [16]. By using electron-beam lithography for

1 μm -long or shorter cells for the horizontal structure in the future, programming power can be reduced. Additionally, dielectric substrates reduce the power losses due to their low thermal conductivities.

3.4 RF Switching

The extracted S parameters of a GeTe resistor (shown in Fig. 1 (c)) are shown in Fig. 5. These parameters were measured in the frequency range of 10 MHz to 20 GHz. In c-GeTe phase, the input reflection coefficient S_{11} was -11 dB which further decreased to -16 dB as the frequency increased from 10 MHz to 20 GHz. This behavior suggests that the reflection in c-GeTe decreases with frequency possibly due to merging of small crystallites at higher frequency which enhances the reflectivity. However, the initial value of insertion loss S_{21} is -3 dB which remains constant with increasing frequency. On the other hand, S_{11} for a-GeTe remains constant in the whole frequency range suggesting 100% return loss. whereas, S_{21} first remains constant to -55 dB in the frequency range of 10-100 MHz followed by steady increase to ending value of -28 dB at 20 GHz. This increasing reflectivity can be attributed to frequency induced crystallization in a-GeTe. In addition, the resistances of the signal line in

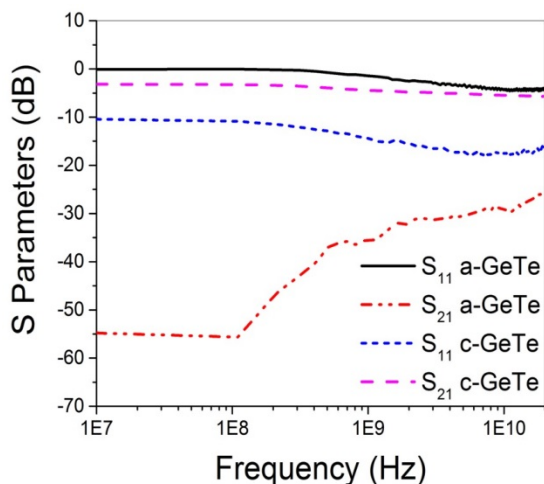


Fig. 5 S parameters of a GeTe RF switch (shown in Fig. 1(c)). In the amorphous phase the signal is strongly reflected, and in the crystalline phase the signal is mostly transmitted. Note that -10 dB and -20 dB correspond to 31.6% and 10% of full signal strength, respectively.

ON and OFF states are 75 Ω and 3.5 M Ω , respectively. By decreasing the width of the cell, a 50 Ω ON state could be achieved, which would minimize S_{21} losses and optimize GeTe for its use as an RF switch. OFF characteristics with 55 dB attenuation up to 100 MHz and ON characteristics with about 5-10 dB attenuation.

4. Conclusion

In this work, the GeTe amorphous-to-crystalline phase transition was investigated using optical, thermal, and electrical methods. Phase change GeTe cells were fabricated by RF sputtering of amorphous GeTe on four types of substrates. The spectroscopic ellipsometry was used to investigate the optical properties of both phases. A sharp increase in n and k GeTe values was observed upon transitioning from amorphous to crystalline phase. The GeTe cells showed six orders of magnitude decrease in resistance as they were heated to their glass temperature. Furthermore, a typical volatile phase change was observed for some PCM cells upon heating them beyond their glass temperature. A cyclical I-V characteristic like memory devices was recorded for samples with a shorter inter-electrode distance. Finally, GeTe cells were demonstrated as an ideal material for RF switches. These results show a wide application range and the volatility of chalcogenide phase change materials which can be engineered by changing the fabrication processes, device dimensions, and choice of substrate.

Acknowledgments

The authors thank the Air Force Office of Scientific Research (AFOSR) for funding this research, and Mr. Brent Danner, Mr. Alex Gwin, and Mr. Christopher Kodama, for their participation.

References

- [1] H. S. Philip Wong, S. Raoux, S. Kim, J. Liang, J. P. Reifenberg, B. Rajendran, M. Asheghi and K. E. Goodson *Phase Change Memory: Proceedings of IEEE 98*, 2010, pp. 2201-2227.

- [2] M. Wuttig and N. Yamada, Phase-change materials for rewriteable data storage, *Nat. Materials* 6 (2007) 824-832.
- [3] T. Ohta, Phase-change optical memory promotes the DVD optical disk, *J. Optoelec. Advan. Mat.* 3 (2001) 609-626.
- [4] A. H. Gwina, C. H. Kodama, T. V. Laurvick, R. A. Coutu, Jr. and P. F. Taday, Improved terahertz modulation using germanium telluride (GeTe) chalcogenide thin films, *Appl. Phys. Lett.* 107 (2015) 031904-031907.
- [5] Y. Shim, G. Hummel and M. Rais-Zadeh, RF switches using phase change materials, in: *IEEE 26th International Conference on MEMS*, 2013, 237-240.
- [6] N. El-Hinnawy et al., A four-terminal, inline, chalcogenide phase-change RF switch using an independent resistive heater for thermal actuation, *IEEE Electron. Dev. Lett.* 34 (2013) 1313.
- [7] G. W. Burr et al., Phase change memory applications, *J. Vac. Sci. Tech. B* 28 (2010) (2) 223-262.
- [8] A. H. Edwards, Theory of persistent, p-type, metallic conduction in c-GeTe, *J. Phys. Condens. Matter* 17 (2005) (32) 329-335.
- [9] A. V. Kolobov and J. Tominaga, Local structure of crystallized GeTe films, *Appl. Phys. Lett.* 82 (2003) (3) 382-384.
- [10] T. Chattopadhyay, J. X. Boucherle and H. G. Schnering, Neutron diffraction study on the structural phase transition in GeTe, *J. Phys. C: Solid State Phys.* 20 (1987) (10) 1431-1440.
- [11] E. M. Levin, M. F. Besser and R. Hanus, Electronic and thermal transport in GeTe: A versatile base for thermoelectric materials, *J. Appl. Phys.* 114 (2013) (8).
- [12] D. Goncalves and E. A. Irene, Fundamentals and applications of spectroscopic ellipsometry, *Quim. Nova* 25 (2002) (5) 794-800.
- [13] G. E. Jellison and F. A. Modine, Parameterization of the optical functions of amorphous materials in the interband region, *Appl. Phys. Lett.* 69 (1996) (3) 371-373.
- [14] M. Gaillet, L. Yan and E. Teboul, Optical characterization of complete TFT-LCD display devices by phase modulated spectroscopic ellipsometry, *Thin Solid Films* 516 (2007) (2-4) 170-174.
- [15] M. Gill, T. Lowrey and J. Park, Ovonic unified memory — A high-performance nonvolatile memory technology for stand-alone memory and embedded applications, *IEEE Intl. Solid-State Circuits*, 2002.
- [16] M. Golio and J. Golio, *RF and Microwave Circuits, Measurements, and Modeling*, Taylor & Francis Group, Boca Raton, FL, 2008.
- [17] Y. A. Çengel, R. H. Turner and J. M. Cimbala, *Fundamentals of Thermal-Fluid Sciences*, McGraw-Hill, New York, NY, 2008.
- [18] S. R. Ovshinsky, Reversible Electrical Switching Phenomena in Disordered Structures, *Phys. Rev. Lett.* 21 (1968) (20) 1450-1453.
- [19] D. Ielmini and Y. Zhang, Analytical model for subthreshold conduction and threshold switching in chalcogenide-based memory devices, *J. Appl. Phys.* 102 (2007) (5).